ACS APPLIED NANO MATERIALS

www.acsanm.org Article

Nanoscale-Thick CuPc/β-Ga_2O_3 p−n Junctions for Harsh-Environment-Resistant Self-Powered Deep-UV Photodetectors

Tianli Zhao, Huaile He, Chao Wu,* Li Lai, Yanxiu Ma, Hu Yang, Haizheng Hu, Aiping Liu, Daoyou Guo, and Shunli Wang*

Cite This: *ACS Appl. Nano Mater.* 2023, 6, 3856−3862 Read Online

ACCESS | Metrics & More | Article Recommendations | Supporting Information

ABSTRACT: Due to their crucial role in ultraviolet communication and monitoring, deep-ultraviolet (DUV) photodetectors have garnered much interest. Recently, Ga_2O_3 has emerged as the best material for DUV photodetectors because of its ultrawide bandgap (4.5−4.9 eV), excellent UV photon absorption coefficient, high structural stability, and affordability. However, there are several difficulties in realizing high-performance Ga_2O_3-based DUV photodetectors with a high tolerance for harsh environments. In this work, nanoscale-thick CuPc/β-Ga_2O_3 p−n junctions were used to build high-performance DUV photodetectors by a straightforward solution-processing approach. The p−n junction photodetectors exhibit improved photoelectric performance compared to a single device made of β-Ga_2O_3 or CuPc, with a photo-to-dark current ratio of 3700 and a fast response time of ∼20 ms under a bias of 0 V. Due to the excellent stability of the nanoscale-thick CuPc film, the device can maintain a high photocurrent even at high temperatures or under long-term DUV irradiation. Our work provides an effective strategy toward highly harsh-environment-resistant DUV photodetectors.

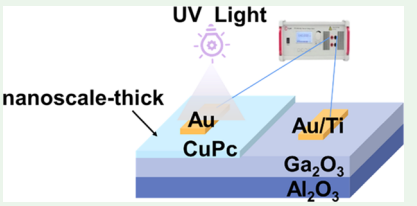

KEYWORDS: *β-Ga_2O_3, CuPc, nanoscale-thick, deep-ultraviolet photodetector, organic−inorganic hybrid heterojunction, harsh-environment-resistant*

INTRODUCTION

As an essential component of spectrum detectors, the deep-ultraviolet (DUV, 200−280 nm) photodetector has a variety of vital uses, including in missile tracking, navigation, communication, and monitoring.[1−4] Despite their low price and maturity in technology, traditional silicon-based DUV photodetectors have limited responsivity to DUV light, a small penetration depth for high-energy ultraviolet photons, and a low filtration dependency on such photons. Recently, wide-bandgap semiconductors such as MgZnO,[5,6] AlGaN,[7,8] diamond,[9−11] and Ga_2O_3[12−18] have been considered alternatives to Si in advanced DUV photodetectors. Ga_2O_3 is the most ideal option for DUV photodetector applications among the numerous wide-bandgap semiconductors because of its ultrawide bandgap (4.5−4.9 eV), strong UV photon absorption coefficient, high structural stability, and affordability.

The structure of a Ga_2O_3-based DUV photodetector is critical to its performance. Initially, the device structure was primarily a photoconductive-type and metal−semiconductor−metal (MSM) structure,[14,19] which has the advantages of simple production and easy integration in device preparation but also has many disadvantages, such as a slow response speed, a small photosensitive area, and the need for an external bias. The self-powered photodetector based on the photovoltaic effect can detect an optical signal without a bias, eliminating the power distribution device and addressing the development needs of energy conservation, which has received broad attention. Ga_2O_3-based self-powered photodetectors with inorganic heterojunctions,[20,21] organic−inorganic hybrid heterojunctions,[22,23] phase junctions,[24,25] and Schottky junctions[26−30] have been reported. Although inorganic heterojunction photodetectors show a high responsivity, inorganic semiconductors with large carrier concentrations have a narrow bandgap and the risk of a light response for non-DUV regions. Some organic molecule materials with strong hole mobility and natural DUV splitting properties are appropriate for building organic−inorganic hybrid self-powered photodetectors with Ga_2O_3. Our previous work used four hole-transport organic materials (TAPC, NPB, CBP, and MCP) to construct heterojunction photodetectors with β-Ga_2O_3. All of the photodetectors demonstrated self-powered characteristics with a low dark current, a high light-to-dark current ratio, high detectivity, and good spectral selectivity.[31] However, the thermal and radiation stability of these organic compounds is poor, limiting their practical use. Copper phthalocyanine (CuPc) has intriguing electrical and optical properties and is widely employed in electronic and optoelectronic devices. Because of its high thermal stability,

Received: December 27, 2022
Accepted: February 14, 2023
Published: February 22, 2023

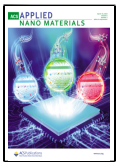

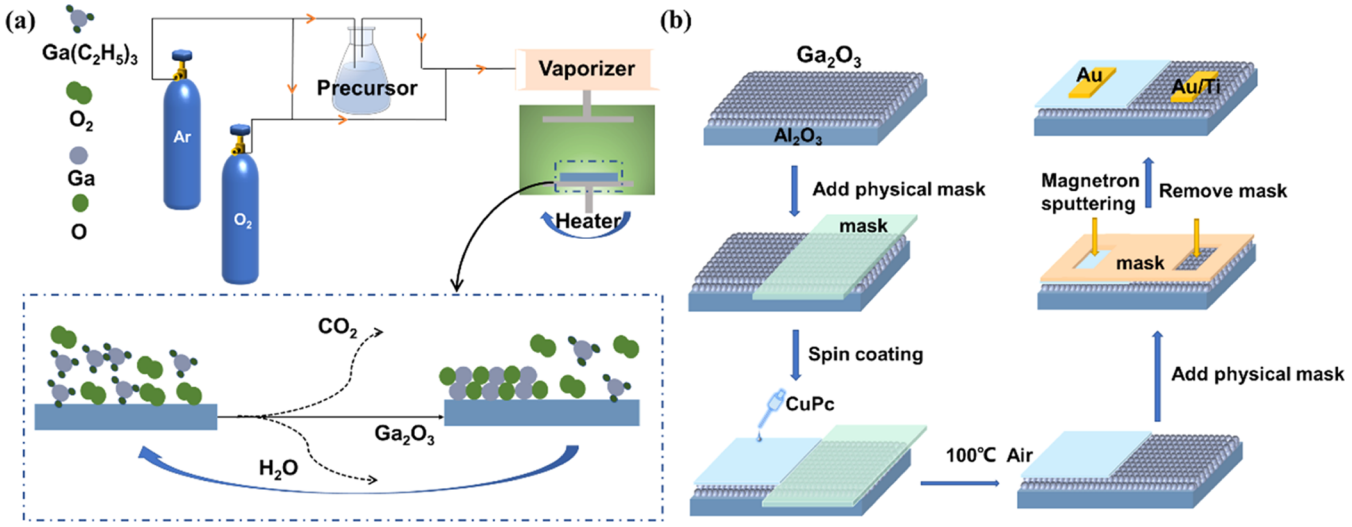

Figure 1. Schematic of (a) synthesis of β-Ga_2O_3 by MOCVD and (b) fabrication of the CuPc/β-Ga_2O_3 p−n junction DUV photodetector.

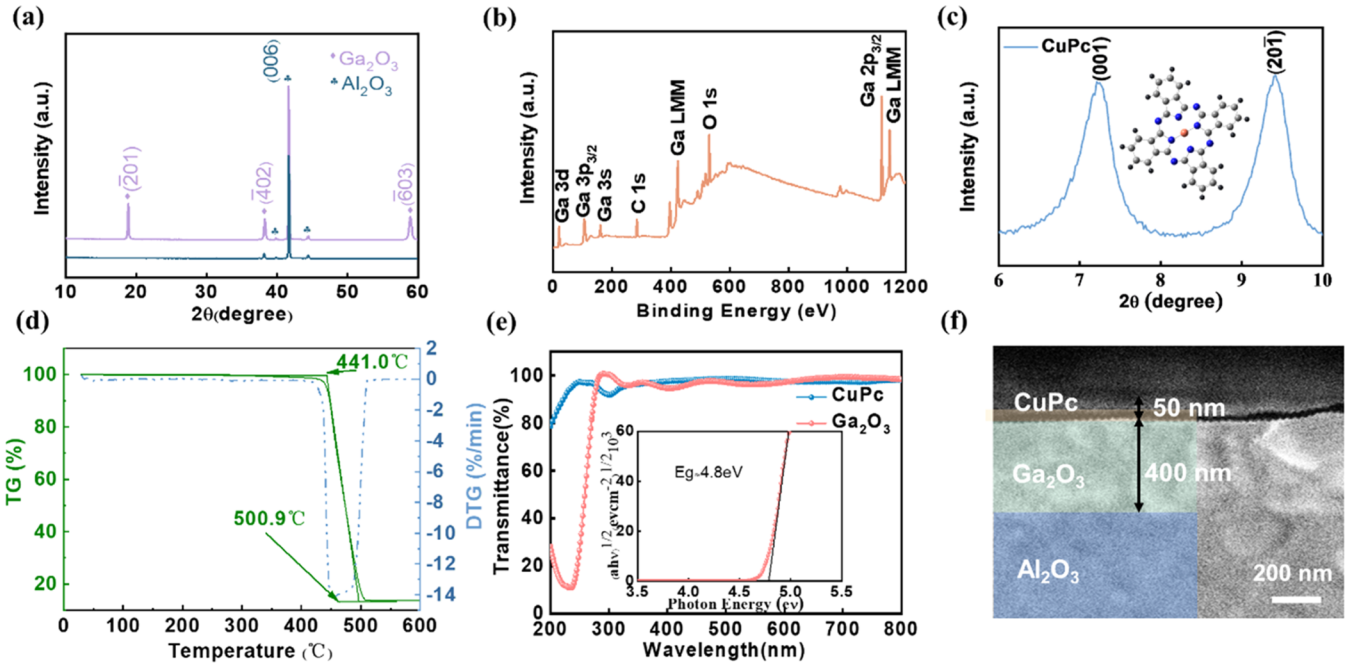

Figure 2. (a) XRD patterns of the β-Ga_2O_3 film; (b) XPS spectra of the β-Ga_2O_3 film; (c) XRD patterns of the nanoscale-thick CuPc film; (d) thermogravimetric analysis of the CuPc film; (e) transmission spectra and bandgap of β-Ga_2O_3 and CuPc films; and (f) SEM image of the CuPc/β-Ga_2O_3 p−n junction.

nanoscale-thick CuPc thin films can remain stable without degradation at high temperatures, unlike other organic compounds. In this work, a nanoscale-thick CuPc film was employed to build a p−n junction photodetector with β-Ga_2O_3 utilizing a simple solution-processing approach. The CuPc unit has facile production pathways, high purity, good solubility, and weak absorption in the UVC region, which can match the requirements of solar-blind photodetectors due to their well-defined molecular architectures. Meanwhile, the high-speed conveyance of photogenerated holes of CuPc and the enormous built-in field obtained from the CuPc/β-Ga_2O_3 p−n junctions provide exceptional optoelectronic performance. The CuPc/β-Ga_2O_3 p−n junction photodetector has an I_{light}/I_{dark} ratio of ∼3700 and a detectivity of 7.8×10^{11} Jones at 0 V. Due to the excellent stability of the nanoscale-thick CuPc film, the device retains excellent sensitivity and stability even in harsh settings such as 150 °C temperatures and continuous irradiation, making it a low-cost, high-performance pursuit for potentially demanding applications.

EXPERIMENTAL SECTION

Preparation of β-Ga_2O_3 Thin Films. Figure 1 shows a schematic diagram of a simple CuPc/β-Ga_2O_3 hybrid-based p−n junction preparation process. First, the β-Ga_2O_3 film is deposited on a (0001) sapphire substrate by the metal−organic chemical vapor deposition (MOCVD) method using oxygen and triethylgallium as reaction precursors. The chemical reaction process of the film preparation is shown in Figure 1a, in which the precursor is adsorbed, migrates, diffuses, and reacts on and desorbs from the surface of the substrate and carbon dioxide and water are removed from the reaction chamber by Ar gas.[32,33] A β-Ga_2O_3 film with a thickness of 400 nm was grown

https://doi.org/10.1021/acsanm.2c05499
ACS Appl. Nano Mater. 2023, 6, 3856−3862

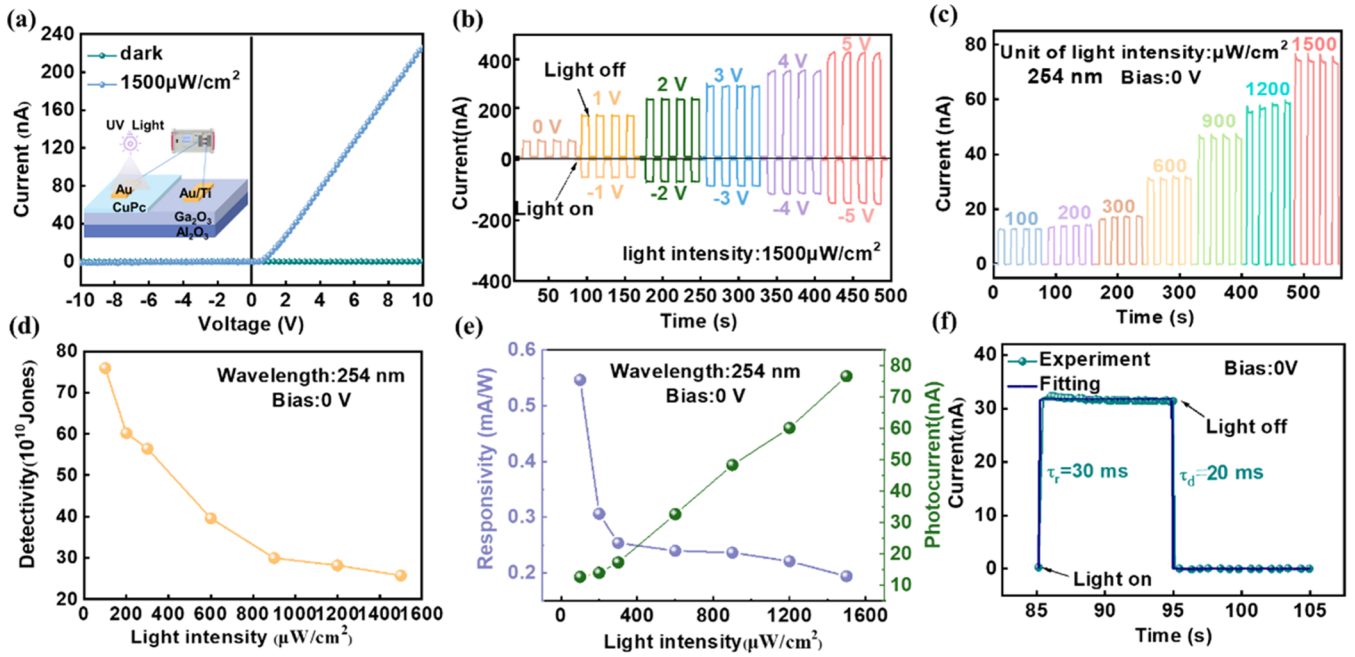

Figure 3. (a) $I-V$ curves of the CuPc/β-Ga_2O_3 p−n junction photodetector under dark and 254 nm light; (b) $I-t$ curves of the CuPc/β-Ga_2O_3 p−n junction photodetector under various bias; (c) $I-t$ curves of the CuPc/β-Ga_2O_3 p−n junction photodetector under 254 nm light with various light intensities; (d) detectivity of the CuPc/β-Ga_2O_3 p−n junction photodetector under 254 nm light with various light intensities; (e) responsivity and photocurrent of the CuPc/β-Ga_2O_3 p−n junction photodetector under 254 nm light with various light intensities; and (f) response speed of the CuPc/β-Ga_2O_3 p−n junction photodetector under 254 nm light with an illumination intensity of 600 $\mu W/cm^2$.

at 860 °C for 1.5 h. Oxygen plasma treatment was used to decrease the oxygen vacancies of the β-Ga_2O_3 photodetector.

Device Preparation Processes. The p-type organic semiconductor CuPc solution was spin-coated on the unmasked area of the Ga_2O_3 film surface and then heated at 100 °C for 20 min to fabricate a nanoscale-thick CuPc/β-Ga_2O_3 hybrid-based p−n junction. Later, the Ti/Au test electrode was created by magnetron sputtering on the β-Ga_2O_3 film, while the Au test electrodes were prepared on the CuPc thin film. A schematic diagram of the cross-sectional device structure is illustrated in Figure S1, and the effective area of the photodetectors is ~0.03 cm^2.

Characterization and Measurement. The surface and cross-sectional morphologies of the prepared CuPc and β-Ga_2O_3 films were studied by scanning electron microscopy (SEM, JSM-5610LV). The transmittance and UV−visible absorption spectra were recorded using a Hitachi U-3900 UV spectrophotometer. A Ta NETZSCH instrument was used to conduct the thermogravimetric test. The photodetector voltage−current ($I-V$) characteristics and the time-dependent optical response ($I-t$) were measured using Keithley 2400 and 6487.

RESULTS AND DISCUSSION

To create high-quality p−n junctions, materials with high crystallinity, strong spectrum selectivity, and good interface interaction are required. The Ga_2O_3 film used in this work exhibits diffraction peaks at 2θ values of 18.8, 38.8, and 58.8°, which demonstrate the creation of crystalline β-Ga_2O_3 (JCPDS 45-1074) with an $(\bar{2}01)$ orientation, as seen in the XRD patterns of Figure 2a. Comparative XPS investigations were carried out, as shown in Figure 2b, to obtain access to information on the material compositions and valence. Due to the poor conductivity of the sample, we did not calibrate the energy scale of the spectrometer, which would have caused the Fermi edge of the sample that remained in electrical contact with the spectrometer to coincide with 0 eV of the BE scale, but instead used the conventional C 1s BE referencing method. As reported by Greczynski et al.,[34] the C 1s peak position varies over an alarmingly large range, from 284.08 to 286.74 eV; hence, the charge reference is usually based on the C 1s peak (284.8 eV) of adventitious carbon, which has recently been proven to be unreliable. Interestingly, the sum of the C 1s binding energy and work function (Φ_A) is constant at 289.58 ± 0.14 eV. Therefore, calibration can be performed by setting the C 1s peak at 289.58 eV. The work function of the Ga_2O_3 material is 4.46 eV, which implies that the C 1s peak at 285.12 eV can be selected. According to the standard value, the peaks of the core levels Ga 2p, O KLL, O 1s, Ga LMM, C 1s, Ga 3s, Ga 3d, and Ga 3p were observed. The crystallinity of the nanoscale-thick CuPc film was also studied by XRD. As shown in Figure 2c, the nanoscale-thick CuPc film is found to be in the β-phase, with typical peaks at 2θ = 7.09 and 9.26°.[35−39] Thermogravimetric analysis (TGA) was carried out from ambient temperature to 600 °C under nitrogen flow to investigate the thermal characteristics of CuPc (Figure 2d). The CuPc begins to decompose at 441 °C, demonstrating that CuPc has excellent thermal stability. The spectral performance of a photodetector is highly related to the absorption by the active material. The nanoscale-thick CuPc film has a larger deep-UV transparent zone in its transmission spectra, suggesting that it has no effect on the absorption by the photosensitive layer of the β-Ga_2O_3 film at these wavelengths (Figure 2e). As seen in the inset, the β-Ga_2O_3 film satisfies the requirement for the optical bandgap of the photosensitive layer of DUV devices, with a value of ~4.80 eV. Figure 2f shows a cross-sectional SEM image of the CuPc/β-Ga_2O_3 junction. The CuPc and β-Ga_2O_3 layers show thicknesses of ~400 and 50 nm, respectively. The border of the nanoscale-thick CuPc layer is uniform, and the β-Ga_2O_3 film does not have any noticeable particle protrusions, which indicates that the β-Ga_2O_3 and CuPc layers have good physical contact and that

https://doi.org/10.1021/acsanm.2c05499
ACS Appl. Nano Mater. 2023, 6, 3856−3862

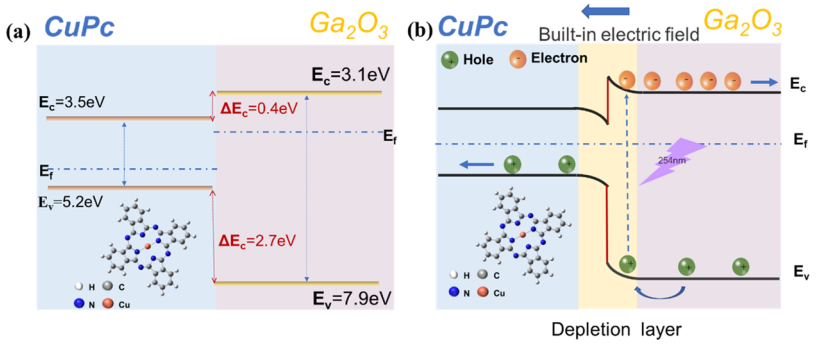

Figure 4. (a) Band structure diagram of the β-Ga_2O_3/CuPc p−n junction photodetector and (b) the charge carrier transport route.

the CuPc/β-Ga_2O_3 heterojunction is acceptable for carrier transfer. Meanwhile, the consistent distributions of Cu, N, O, and Ga suggest that the nanoscale-thick CuPc film is evenly covered on the Ga_2O_3 surface (Figure S2).

After optimizing the spin-coating process (Figure S3), a CuPc/β-Ga_2O_3 p−n junction photodetector was obtained, and its photoelectric properties were studied. The I−V curves of the photodetector were tested first to characterize the photoelectric conversion performance of the photodetector. As shown in Figure 3a, the photodetector exhibits a strong photoresponse and apparent rectifying properties under 254 nm light, with an off-state current of less than 10^{-9} A at −10 V and an on-state current of $\sim 10^{-7}$ A at 10 V, which suggests typical p−n photodiode behavior. Due to the ultrahigh intrinsic resistance (~TΩ) and high crystalline quality of the Ga_2O_3 epitaxial film, there are not enough charge carriers to form an obvious rectifying current under dark conditions; hence, the I−V curves of the device under dark conditions are nearly symmetric. Metal−semiconductor−metal (MSM) devices made from single β-Ga_2O_3 or CuPc were manufactured, and their electrical properties were further tested to demonstrate the origin of the rectifying feature of the device. The linear I−V relationship of the Ti/Au−β-Ga_2O_3−Ti/Au and Au−CuPc−Au structures in Figure S4 confirms the Ohmic contact between β-Ga_2O_3 and the Ti/Au electrode as well as CuPc and the Au electrode. Hence, the outstanding rectifying quality of the heterostructure is solely due to the interface produced between the two materials. An investigation was also performed to determine how the imposed biases affect the photoresponse. Figure 3b depicts the time-dependent photoresponses observed under 254 nm irradiation with a 1500 μW/cm^2 light intensity density and various applied biases. As the applied bias increases, the dark current and the photocurrent increase. The photoresponse curve was fitted with a biexponential relaxation equation to quantitatively describe the current increase and decay process for a more in-depth response time comparison (Figure S5 and Table S1). The rise time decreases with increasing bias, which is due to the ability of the higher electric field to transport more carriers. It is worth noting that, at 0 V, the current rapidly increases under 254 nm irradiation, with a ratio of ~3700, exhibiting a self-powered characteristic. The self-powered feature meets the requirements of today's society for low-power devices, and we measured the optoelectronic performance under the self-powered mode in detail. Figure 3c illustrates the I−t curves of the photodetector in the self-powered mode under various light intensities. The photodetector displays a steady and rapid reaction to changing light intensity density. A sharp spike was observed in the current under a power density higher than 900 μW/cm^2. This phenomenon is very common in β-Ga_2O_3-based optoelectronic devices and is caused by the initial electron−hole pair separation in the depletion layer and/or the local capacitance effects. All of the dynamic responses point to the fact that the p−n junction photodetector can operate with high consistency and repeatability. Both the responsivity (R) and the detectivity (D) of photodetectors are crucially significant factors. Under a light intensity density of 100 mW/cm^2 at 254 nm, the R and D values of the β-Ga_2O_3/CuPc p−n junction photodetector reach their highest levels, 0.55 mA/W and 7.8×10^{11} Jones, respectively (Figure 3d,e). The trap states being filled at higher power intensities may be ascribed to the nonlinear correlation between the photocurrent and power intensity. It is worth noting that the β-Ga_2O_3/CuPc photodetector exhibits a nonlinear photocurrent as a function of light intensity, which can be well fitted by the following equation:

$$I_{ph} \propto P^{\gamma}$$

where P is the light intensity and γ is a factor. γ is <1 owing to the recombination and trapping by oxygen vacancy traps of electron−hole pairs in the β-Ga_2O_3 film. The I−t characteristics varying with the power intensity (less than 10 μW/cm^2) are shown in Figure S6. The photocurrents correspondingly increase as the power intensity increases from 0.1 to 10 μW/cm^2. According to the calculated power law, the exponent value is 0.94, suggesting a linear relationship between the light intensity and light current at low power. The rise time (τ_r) and decay time (τ_d) of the β-Ga_2O_3/CuPc p−n junction photodetector are measured to be 30 and 20 ms, respectively, indicating that the building of the p−n junction can effectively enhance the response speed (Figure 3f). Figure S7 displays the photodetector performance characteristics for a pure β-Ga_2O_3-based device under 254 nm light and a 1 V bias. The response time for the β-Ga_2O_3-based photodetector is 1.46/0.15 s. The CuPc/β-Ga_2O_3 photodetector has a quick response time compared to the pure β-Ga_2O_3-based photodetector because of the heterojunction and the comparatively high hole mobility of CuPc. Between the responsivity and response time, there is a significant trade-off. The Ga_2O_3-based photoconductive gain is mostly due to the trapping of holes close to oxygen vacancies, which improves the photodetector responsivity. More study is required in this area to develop novel strategies for enhancing both responsivity and response time. As a means of elucidating the underlying physical process, the energy band diagram of the CuPc/β-Ga_2O_3 p−n junction photodetector is shown in Figure 4, which forms an example of a type I heterojunction including a straddling gap. When the energy of

https://doi.org/10.1021/acsanm.2c05499
ACS Appl. Nano Mater. 2023, 6, 3856−3862

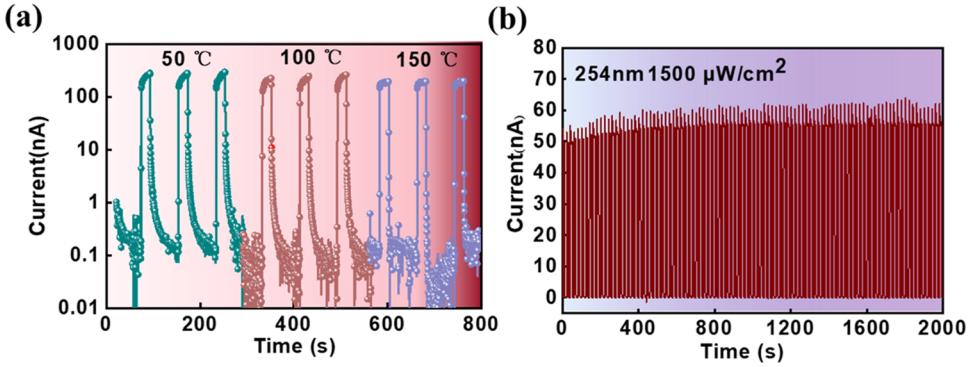

Figure 5. (a) Time-dependent photoresponse of the device working at 50, 100, and 150 °C. (b) Stability measurement of the device after long-time irradiation.

the photon (h_c/λ) is greater than the E_g of Ga_2O_3, the electrons in the ground state of the VB are stimulated, and they jump into the CB, which contributes to the photoconductive effect. Most photons in the depletion zone are used up to produce electron−hole pairs, which are subsequently separated by the driving force of E_0, making the photovoltaic effect possible. The nanoscale-thick CuPc film has a high electron transport efficiency, creates an expressway for the transport of electrons, lowers the recombination rate, and improves the photoelectric detection performance. These exceptional performances of the photodetector can be attributed to the high electron transport efficiency of CuPc and the substantial built-in field present in the p−n junction. Space exploration, flame detection, and combustion monitoring applications strongly require highly developed deep-UV photodetectors that can perform admirably in challenging environments. We researched the CuPc/β-Ga_2O_3 p−n junction photodetector performance in challenging environments due to its exceptional advantages, including under long-term irradiation and high temperatures. As shown in Figure 5, the device maintains its high photoresponse performance at a temperature of 280 °C and under long-term irradiation of 2000 s. The above photoelectronic performance proved that the CuPc/β-Ga_2O_3 p−n junction photodetector performs well in harsh environments.

CONCLUSIONS

A CuPc/β-Ga_2O_3 p−n junction DUV photodetector with excellent self-powered performance was proposed. The CuPc/β-Ga_2O_3 p−n junction effectively promotes the automatic separation of photogenerated carriers, avoiding recombination. At 0 V, the photodetector shows high R and D values of ∼0.55 mA/W and 7.8×10^{11} Jones, respectively, with a fast response time of ∼20 ms. Meanwhile, due to the outstanding stability of the nanoscale-thick CuPc, the device can work under a harsh environment and can maintain a high photocurrent under high temperatures and long-term irradiation.

ASSOCIATED CONTENT

Supporting Information

The Supporting Information is available free of charge at https://pubs.acs.org/doi/10.1021/acsanm.2c05499.

Schematic of the cross-sectional device, SEM images, EDX mapping, linear $I-V$ plots, $I-t$ plots, and response time analysis table (PDF)

AUTHOR INFORMATION

Corresponding Authors

Chao Wu − *Center for Optoelectronics Materials and Devices & Key Laboratory of Optical Field Manipulation of Zhejiang Province, Department of Physics, Zhejiang Sci-Tech University, Hangzhou 310018, China;* orcid.org/0000-0003-2761-8946; Email: chaowu@zstu.edu.cn

Shunli Wang − *Center for Optoelectronics Materials and Devices & Key Laboratory of Optical Field Manipulation of Zhejiang Province, Department of Physics, Zhejiang Sci-Tech University, Hangzhou 310018, China*; Email: slwang@zstu.edu.cn

Authors

Tianli Zhao − *Center for Optoelectronics Materials and Devices & Key Laboratory of Optical Field Manipulation of Zhejiang Province, Department of Physics, Zhejiang Sci-Tech University, Hangzhou 310018, China*

Huaile He − *Center for Optoelectronics Materials and Devices & Key Laboratory of Optical Field Manipulation of Zhejiang Province, Department of Physics, Zhejiang Sci-Tech University, Hangzhou 310018, China*

Li Lai − *Center for Optoelectronics Materials and Devices & Key Laboratory of Optical Field Manipulation of Zhejiang Province, Department of Physics, Zhejiang Sci-Tech University, Hangzhou 310018, China*

Yanxiu Ma − *Center for Optoelectronics Materials and Devices & Key Laboratory of Optical Field Manipulation of Zhejiang Province, Department of Physics, Zhejiang Sci-Tech University, Hangzhou 310018, China*

Hu Yang − *Center for Optoelectronics Materials and Devices & Key Laboratory of Optical Field Manipulation of Zhejiang Province, Department of Physics, Zhejiang Sci-Tech University, Hangzhou 310018, China*

Haizheng Hu − *Center for Optoelectronics Materials and Devices & Key Laboratory of Optical Field Manipulation of Zhejiang Province, Department of Physics, Zhejiang Sci-Tech University, Hangzhou 310018, China*

Aiping Liu − *Center for Optoelectronics Materials and Devices & Key Laboratory of Optical Field Manipulation of Zhejiang Province, Department of Physics, Zhejiang Sci-Tech University, Hangzhou 310018, China;* orcid.org/0000-0002-2338-062X

Daoyou Guo − *Center for Optoelectronics Materials and Devices & Key Laboratory of Optical Field Manipulation of Zhejiang Province, Department of Physics, Zhejiang Sci-Tech*

https://doi.org/10.1021/acsanm.2c05499
ACS Appl. Nano Mater. 2023, 6, 3856−3862

University, Hangzhou 310018, China; orcid.org/0000-0002-6191-1655

Complete contact information is available at: https://pubs.acs.org/10.1021/acsanm.2c05499

Notes

The authors declare no competing financial interest.

■ ACKNOWLEDGMENTS

This work was supported by the National Natural Science Foundation of China (No. 62274148), Fund of the Innovation Center of Radiation Application (No. KFZC202102040), Natural Science Foundation of Zhejiang Province (No. LY20F040005), and Science Foundation of Zhejiang Sci-Tech University (No. 20062224-Y).

■ REFERENCES

(1) Kaur, D.; Kumar, M. A strategic review on gallium oxide based deep-ultraviolet photodetectors: recent progress and future prospects. *Adv. Opt. Mater.* **2021**, *9*, No. 2002160.

(2) Hou, X.; Zou, Y.; Ding, M.; Qin, Y.; Zhang, Z. X.; Ma, P.; Tan, S.; Yu, X.; Zhou, X.; Zhao, G.; Xu, H.; Sun, S. Review of polymorphous Ga_2O_3 materials and their solar-blind photodetector applications. *J. Phys. D: Appl. Phys.* **2021**, *54*, No. 043001.

(3) Zhou, C. Q.; Ai, Q.; Chen, X.; Gao, X. H.; Liu, K. W.; Shen, D. Z. Ultraviolet photodetectors based on wide bandgap oxide semiconductor films. *Chin. Phys. B* **2019**, *28*, No. 048503.

(4) Wu, C.; Wu, F.; Hu, H.; Wang, S.; Liu, A.; Guo, D. Review of self-powered solar-blind photodetectors based on Ga_2O_3. *Mater. Today Phys.* **2022**, *28*, No. 100883.

(5) Chen, H.; Ma, X.; Zhang, J.; Li, Q.; Liu, H.; Chen, Z.; Chu, G.; Chu, S. Avalanche solar blind photodetectors with high responsivity based on MgO/MgZnO heterostructures. *Opt. Mater. Express* **2018**, *8*, 785−793.

(6) Alema, F.; Hertog, B.; Ledyaev, O.; Miller, R.; Osinsky, A.; Schoenfeld, W. V. Temperature and pulse duration effects on the growth of MgZnO via pulsed metal organic chemical vapor deposition. *Jpn. J. Appl. Phys.* **2016**, *55*, No. 035501.

(7) Wang, D.; Huang, C.; Liu, X.; Zhang, H.; Yu, H.; Fang, S.; Ooi, B. S.; Mi, Z.; He, J. H.; Sun, H. Highly Uniform. Self-assembled AlGaN nanowires for self-powered solar-blind photodetector with fast-response speed and high responsivity. *Adv. Opt. Mater.* **2020**, *9*, No. 2000893.

(8) Zhang, W.; Xu, J.; Ye, W.; Li, Y.; Qi, Z.; Dai, J.; Wu, Z.; Chen, C.; Yin, J.; Li, J.; Jiang, H.; Fang, Y. High-performance AlGaN metal−semiconductor−metal solar-blind ultraviolet photodetectors by localized surface plasmon enhancement. *Appl. Phys. Lett.* **2015**, *106*, No. 021112.

(9) Lin, C.-N.; Lu, Y.-J.; Yang, X.; Tian, Y.-Z.; Gao, C.-J.; Sun, J.-L.; Dong, L.; Zhong, F.; Hu, W.-D.; Shan, C.-X. Diamond-based all-carbon photodetectors for solar-blind imaging. *Adv. Opt. Mater.* **2018**, *6*, No. 1800068.

(10) Chen, Y.-C.; Lu, Y.-J.; Lin, C.-N.; Tian, Y.-Z.; Gao, C.-J.; Dong, L.; Shan, C.-X. Self-powered diamond/β-Ga_2O_3 photodetectors for solar-blind imaging. *J. Mater. Chem. C* **2018**, *6*, 5727−5732.

(11) Wei, M.; Yao, K.; Liu, Y.; Yang, C.; Zang, X.; Lin, L. A solar-blind uv detector based on graphene-microcrystalline diamond heterojunctions. *Small* **2017**, *13*, No. 1701328.

(12) Wu, C.; Qiu, L.; Li, S.; Guo, D.; Li, P.; Wang, S.; Du, P.; Chen, Z.; Liu, A.; Wang, X.; Wu, H.; Wu, F.; Tang, W. High sensitive and stable self-powered solar-blind photodetector based on solution-processed all inorganic $CuMO_2/Ga_2O_3$ pn heterojunction. *Mater. Today Phys.* **2021**, *17*, No. 100335.

(13) Pintor-Monroy, M. I.; Barrera, D.; Murillo-Borjas, B. L.; Ochoa-Estrella, F. J.; Hsu, J. W.; Quevedo-Lopez, P. M. A. Tunable electrical and optical properties of nickel oxide (NiO_x) thin films for fully transparent NiO_x-Ga_2O_3 p-n junction diodes. *ACS Appl. Mater. Interfaces* **2018**, *10*, 38159−38165.

(14) Oh, S.; Kim, C.-K.; Kim, J. High responsivity β-Ga_2O_3 metal-semiconductor-metal solar-blind photodetectors with ultraviolet transparent graphene electrodes. *ACS Photonics* **2018**, *5*, 1123−1128.

(15) Mahmoud, W. E. Solar blind avalanche photodetector based on the cation exchange growth of β-Ga_2O_3/SnO_2 bilayer heterostructure thin film. *Sol. Energy Mater. Sol. Cells* **2016**, *152*, 65−72.

(16) Li, Y.; Tokizono, T.; Liao, M.; Zhong, M.; Koide, Y.; Yamada, I.; Delaunay, J.-J. Efficient assembly of bridged β-Ga_2O_3 nanowires for solar-blind photodetection. *Adv. Funct. Mater.* **2010**, *20*, 3972−3978.

(17) Hou, X.; Zhao, X.; Zhang, Y.; Zhang, Z.; Liu, Y.; Qin, Y.; Tan, P.; Chen, C.; Yu, S.; Ding, M.; Xu, G.; Hu, Q.; Long, S. High-Performance harsh-environment-resistant GaO_X solar-blind photodetectors via defect and doping engineering. *Adv. Mater.* **2021**, *34*, No. 2106923.

(18) Wu, C.; Wu, F.; Deng, L.; Li, S.; Wang, S.; Cheng, L.; Liu, A.; Wang, J.; Tang, W.; Guo, D. Solution-processed Y-doped $SnSrO_3$ electron transport layer for Ga_2O_3 based heterojunction solar-blind photodetector with high sensitivity. *Vacuum* **2022**, *201*, No. 111064.

(19) Zhou, H.; Cong, L.; Ma, J.; Li, B.; Chen, M.; Xu, H.; Liu, Y. High gain broadband photoconductor based on amorphous Ga_2O_3 and suppression of persistent photoconductivity. *J. Mater. Chem. C* **2019**, *7*, 13149−13155.

(20) Yu, J.; Yu, M.; Wang, Z.; Yuan, L.; Huang, Y.; Zhang, L.; Zhang, Y.; Jia, R. Improved photoresponse performance of self-powered β-Ga_2O_3/NiO heterojunction uv photodetector by surface plasmonic effect of Pt nanoparticles. *IEEE Trans. Electron Devices* **2020**, *67*, 3199−3204.

(21) Wu, Z.; Jiao, L.; Wang, X.; Guo, D.; Li, W.; Li, L.; Huang, F.; Tang, W. A self-powered deep-ultraviolet photodetector based on an epitaxial Ga_2O_3/Ga:ZnO heterojunction. *J. Mater. Chem. C* **2017**, *5*, 8688−8693.

(22) Zhang, D.; Zheng, W.; Lin, R.; Li, Y.; Huang, F. Ultrahigh EQE (15%) Solar-blind uv photovoltaic detector with organic-inorganic heterojunction via dual built-in fields enhanced photogenerated carrier separation efficiency mechanism. *Adv. Funct. Mater.* **2019**, *29*, No. 1900935.

(23) Wang, Y.; Li, L.; Wang, H.; Su, L.; Chen, H.; Bian, W.; Ma, J.; Li, B.; Liu, Z.; Shen, A. An ultrahigh responsivity self-powered solar-blind photodetector based on a centimeter-sized beta-Ga_2O_3/polyaniline heterojunction. *Nanoscale* **2020**, *12*, 1406−1413.

(24) Wu, C.; He, C.; Guo, D.; Zhang, F.; Li, P.; Wang, S.; Liu, A.; Wu, F.; Tang, W. Vertical α/β-Ga_2O_3 phase junction nanorods array with graphene-silver nanowire hybrid conductive electrode for high-performance self-powered solar-blind photodetectors. *Mater. Today Phys.* **2020**, *12*, No. 100193.

(25) Wang, Y.; Cui, W.; Yu, J.; Zhi, Y.; Li, H.; Hu, Z. Y.; Sang, X.; Guo, E. J.; Tang, W.; Wu, Z. One-Step growth of amorphous/crystalline Ga_2O_3 phase junctions for high-performance solar-blind photodetection. *ACS Appl. Mater. Interfaces* **2019**, *11*, 45922−45929.

(26) Yang, C.; Liang, H.; Zhang, Z.; Xia, X.; Tao, P.; Chen, Y.; Zhang, H.; Shen, R.; Luo, Y.; Du, G. Self-powered SBD solar-blind photodetector fabricated on the single crystal of β-Ga_2O_3. *RSC Adv.* **2018**, *8*, 6341−6345.

(27) Wang, Y.; Yang, Z.; Li, H.; Li, S.; Zhi, Y.; Yan, Z.; Huang, X.; Wei, X.; Tang, W.; Wu, Z. Ultrasensitive flexible solar-blind photodetectors based on graphene/amorphous Ga_2O_3 van der waals heterojunctions. *ACS Appl. Mater. Interfaces* **2020**, *12*, 47714−47720.

(28) Suzuki, R.; Nakagomi, S.; Kokubun, Y.; Arai, N.; Ohira, S. Enhancement of responsivity in solar-blind β-Ga_2O_3 photodiodes with a Au Schottky contact fabricated on single crystal substrates by annealing. *Appl. Phys. Lett.* **2009**, *94*, No. 222102.

(29) Pratiyush, A. S.; Xia, Z.; Kumar, S.; Zhang, Y.; Joishi, C.; Muralidharan, R.; Rajan, S.; Nath, D. N. MBE-grown β-Ga2O3-based schottky uv-c photodetectors with rectification ratio ~10^7. *IEEE Photonics Technol. Lett.* **2018**, *30*, 2025−2028.

(30) Mukhopadhyay, P.; Schoenfeld, W. V. High responsivity tin gallium oxide Schottky ultraviolet photodetectors. *J. Vac. Sci. Technol. A* **2020**, *38*, No. 013403.
(31) Wu, C.; Wu, F.; Ma, C.; Li, S.; Liu, A.; Yang, X.; Chen, Y.; Wang, J.; Guo, D. A general strategy to ultrasensitive Ga_2O_3 based self-powered solar-blind photodetectors. *Mater. Today Phys.* **2022**, *23*, No. 100643.
(32) Li, S.; Yue, J.; Yan, Z.; Liu, Z.; Lu, C.; Li, P.; Guo, D.; Wu, Z.; Guo, Y.; Tang, W. Enhancing the self-powered performance in VO_x/Ga_2O_3 heterojunction ultraviolet photodetector by hole-transport engineering. *J. Alloys Compd.* **2022**, *902*, No. 163801.
(33) Li, S.; Guo, D.; Li, P.; Wang, X.; Wang, Y.; Yan, Z.; Liu, Z.; Zhi, Y.; Huang, Y.; Wu; Tang, Z. W. Ultrasensitive, Superhigh Signal-to-Noise Ratio, Self-Powered Solar-Blind Photodetector Based on n-Ga_2O_3/p-CuSCN Core-Shell Microwire Heterojunction. *ACS Appl. Mater. Interfaces* **2019**, *11*, 35105−35114.
(34) Greczynski, G.; Hultman, L. X-ray photoelectron spectroscopy: Towards reliable binding energy referencing. *Prog. Mater. Sci.* **2020**, *107*, 100591.
(35) Peng, Fei.; Qin, S. J.; Hu, L. F.; Wang, J. Y.; Yang, J. M.; Chen, X. Q.; Pan, G. B. Electrochemical fabrication and optoelectronic properties of hybrid heterostructure of CuPc/porous GaN. *Chem. Phys. Lett.* **2016**, *652*, 6−10.
(36) Tatar, B.; Demiroglu, D.; Urgen, M. Investigation of structural and electrical properties of p-CuPc/c-Si and p-CuPc/a-Si/c-Si hybrid photodiodes prepared by CSP technique. *Microelectron. Eng.* **2014**, *126*, 184−190.
(37) Jana, A.; Kumari, K.; Dey, A.; Reddy, P. S. S.; Biswas, B.; Gupta, B.; Sarkar, S. K. Fabrication of P-N heterojunction based MoS2 modified CuPc nanoflowers for humidity sensing. *Sens. Actuators, A* **2019**, *299*, No. 111574.
(38) Ullah, I.; Shah, M.; Khattak, S. A.; Khan, G. Temperature effect on electronic parameters of CuPc/n-Si heterojunction. *J. Electron. Mater.* **2019**, *48*, 5609−5616.
(39) Chen, Q. H.; Ding, Y.; Wu, Y. K.; Sui, M. Q.; Lu, W.; Wang, B.; Su, W. M.; Cui, Z.; Chen, L. W. Passivation of surface states in the ZnO nanowire with thermally evaporated copper phthalocyanine for hybrid photodetectors. *Nanoscale* **2013**, *5*, 4162−4165.

https://doi.org/10.1021/acsanm.2c05499
ACS Appl. Nano Mater. 2023, 6, 3856−3862